ELSEVIER

Cardiovascular Research 56 (2002) 248–259

Cardiovascular Research

www.elsevier.com/locate/cardiores

Structural and functional implications of the phospholamban hinge domain: impaired SR Ca^{2+} uptake as a primary cause of heart failure

Albrecht G. Schmidt[a,1], Jing Zhai[a,1], Andrew N. Carr[a], Mike J. Gerst[a], John N. Lorenz[b], Piero Pollesello[c], Arto Annila[d], Brian D. Hoit[e], Evangelia G. Kranias[a,*]

[a]*Department of Pharmacology and Cell Biophysics, University of Cincinnati College of Medicine, 231 Albert Sabin Way, Cincinnati, OH 45267-0575, USA*

[b]*Department of Molecular and Cellular Physiology, University of Cincinnati College of Medicine, Cincinnati, OH 45267, USA*

[c]*Cardiovascular Research, Orion Pharma, FIN-02101 Espoo, Finland*

[d]*VTT Biotechnology, FIN-00014 Helsinki, Finland*

[e]*Division of Cardiology, Case Western Reserve University, Cleveland, OH 44106, USA*

Received 20 March 2002; accepted 17 June 2002

Abstract

Objective: The role of sarcoplasmic reticulum (SR) in the onset and progression of heart failure is controversial. We tested the hypothesis that impairment of SR Ca^{2+} sequestration may be a primary cause for progressive left ventricular (LV) dysfunction and the phospholamban hinge domain may be critical in this process. **Methods:** A phospholamban hinge domain mutant (PLB/N27A) was introduced in the cardiac compartment of the phospholamban null mouse. An integrative approach was used to characterize the resulting cardiac phenotype at a structural, cellular, whole organ and intact animal level. **Results:** NMR analysis revealed a defined alteration in the α-helical configuration between residues Q22 to F35 in mutant phospholamban. Transgenic lines expressing similar levels of mutant compared to wild-type phospholamban exhibited super-inhibition of the SR Ca^{2+} ATPase affinity for Ca^{2+} (EC_{50} 0.52 μM) in oxalate-supported Ca^{2+} uptake measurements, which translated into impaired relaxation and attenuated responses to β-adrenergic stimulation. Importantly, a blunted force–frequency relation was observed in mutant hearts preceding left ventricular dilation. Upon aging to 10 months, the predominantly diastolic dysfunction progressed to congestive heart failure, characterized by induction of a fetal gene program, cardiac remodeling, lung congestion, depressed systolic function and early mortality. **Conclusion:** Increased inhibition of Ca^{2+} sequestration may be a causative factor in the development of left ventricular dysfunction and myocyte remodeling leading to heart failure. Furthermore, the hinge domain may play an important role in transmitting PLB's regulatory effects on SERCA.

Keywords: Ca-pump; Calcium (cellular); Contractile function; Heart failure; SR (function)

1. Introduction

Dilated cardiomyopathy represents a final common pathway in response to a variety of different pathologic stimuli and reflects the complex interaction of cascades that drive the onset and progression of the disease. At the functional level, end-stage heart failure is commonly associated with depression of systolic performance [1] and marked diastolic dysfunction [2]. Although there is now evidence that diastolic dysfunction may represent the early phase of heart failure preceding systolic impairment [2], the effectors and cellular mechanisms that underlie impaired myocardial relaxation and its transition to congestive heart failure have not been well defined.

Studies in human and animal models of heart failure have suggested that the elevated resting [Ca^{2+}] and prolonged duration of the Ca^{2+} transient [3–5] are primari-

*Corresponding author. Tel.: +1-513-558-2327; fax: +1-513-558-2269.

E-mail address: litsa.kranias@uc.edu (E.G. Kranias).

[1]Each author contributed equally to this manuscript.

Time for primary review 26 days.

0008-6363/02/$ – see front matter
PII: S0008-6363(02)00541-2

ly due to impaired Ca^{2+} sequestration by the SR. However, other Ca^{2+} regulatory mechanisms, such as blunted myofilament activation [6], impaired ability of L-type Ca-channel to activate SR Ca^{2+} release [7], dysfunction of the ryanodine receptor [8], or abnormalities in myocyte cytoskeleton [9] may contribute to the disturbed Ca homeostasis. Furthermore, it has been postulated that depressed SR Ca function may be an important compensatory response to minimize contractile depression and preserve energy expenditure [6]. Unfortunately, the pleiotropic factors leading to heart failure and the complex phenotype characterizing the end stages, limit our ability to distinguish between primary causes and secondary adaptive responses.

Cardiac relaxation is critically dependent on the activity of the SR Ca^{2+} ATPase (SERCA), which is under reversible regulation by phospholamban (PLB) [10,11]. Dephosphorylated PLB inhibits SERCA's Ca^{2+} affinity, whereas phosphorylation by cAMP-dependent and Ca^{2+}/calmodulin-dependent protein kinases, relieves this inhibition [12]. The inhibitory effects of PLB involve amino acids (AA) in the hydrophobic transmembrane domain II (AA 31–52) and in cytosolic domain Ia (AA 1–20) [13,14]. Domain Ib (AA 21–30), a hinge region in the cytosolic portion of PLB, has been suggested to regulate a long range coupling between domains Ia and II [15], but its functional significance is not clear. The role of PLB in the regulation of cardiac function has been elucidated through the characterization of genetically altered mouse models. Ablation of PLB resulted in hyperdynamic contractile parameters, while PLB overexpression led to significantly depressed function [10,11]. Furthermore, overexpression of PLB or mutants, which act as gain-of-function inhibitors, indicated that depressed SR Ca^{2+} cycling was associated with hypertrophy [16,17]. Thus, it is interesting to postulate that PLB may be a control point in the regulation of intracellular Ca^{2+} dynamics and myocyte adaptive responses to compensatory hypertrophy. However, interpretation of the PLB overexpression studies is rather limiting since they are done in the presence of the endogenous wild-type molecule, and it is difficult to discern between the effects of mass action or mutation. Furthermore, the overexpressed mutant may either coexist with the endogenous protein or may disrupt the regulatory effects of the wild-type molecule, leading to the observed phenotype.

Thus, we introduced an Asn^{27} to Ala (N27A) PLB mutant, which acts as a superinhibitor of SERCA while maintaining its native pentameric structure, in the cardiac compartment of the null background. In the present study, we have characterized structural alterations and the primary functional effects of this hinge region mutant on SERCA2a activity, basal contractility, Ca^{2+} handling, β-adrenergic responsiveness and contractile reserve in vitro and in vivo. Furthermore, we have used this animal model to assess the pathophysiological significance of chronic impairment of SR Ca^{2+} resequestration for the onset and progression of heart failure.

2. Methods

2.1. Introduction of the PLB/N27A mutant into the PLB null background

Transgenic mice, overexpressing the PLB/N27A mutant (FVB/N) [17] were crossbred with the PLB knockout mice (129X1/SvJ×CF-1) [10]. PCR methodology was employed to identify offspring expressing both the PLB/N27A transgene and the *neo* gene [10,17]. The transgenic construct was also subjected to sequencing to confirm the presence of the PLB Asn^{27} to Ala mutation (AAT to GCT) and the absence of additional mutations in the coding region of the PLB cDNA. Characterization studies utilized mice from the F_4 generation. Wild-type mice with 129X1/SvJ×CF-1 mixed background were used as controls. The investigation conforms with the *Guide for the Care and Use of Laboratory Animals* published by the US National Institutes of Health (NIH Publication No. 85-23, revised 1996).

2.2. Biochemical assays

Crude cardiac homogenates and SR enriched microsomes [17] were subjected to quantitative immunoblotting [18]. Phosphorylation assays were conducted as previously described [19]. Oxalate-supported Ca^{2+} uptake in SR was measured by a modified Millipore filtration technique, and data were analyzed by nonlinear regression using Origin software [17].

2.3. Structural NMR-analysis

Wild-type and mutant N27A PLB peptides (AA 1–36) were synthesized, purified [20], and two-dimensional proton correlation NMR spectra were acquired from 1 mM samples dissolved in 30% TFE at pH 3.0, 17 °C, using an 800 MHz NMR spectrometer [21]. Structures were generated by torsion angle simulated annealing (DYANA 1.5) [22]. Families of structures were analyzed for restraint violation, backbone dihedral (Ramachandran plot), energy and root mean square deviation.

2.4. Ventricular cardiomyocyte mechanical parameters and Ca^{2+} transient measurements

Ca^{2+}-tolerant, isolated cardiomyocytes were loaded with 3–5 μM Fura 2-AM for 20 min at room temperature. Cardiomyocytes were perfused with 1.8 mM Ca^{2+}-Tyrode and field-stimulated at 0.5 Hz in the absence or presence of isoproterenol (300 nM). Ca^{2+} transients were measured as the 340/380 nm fluorescence ratio and reported in arbitrary units [18].

2.5. Langendorff heart perfusion

Retrograde aortic Langendorff perfusion was performed using modified Krebs buffer saturated with 95% O_2–5% CO_2 at 37 °C [19]. Hearts were frozen upon maximal isoproterenol stimulation (1.0 μM), and subjected to Western blot analysis or SR Ca^{2+} uptake measurements.

2.6. Closed-chest catheterization and force–frequency relation

Left ventricular (LV) catheterization was performed using a 1.4 Fr Millar high fidelity catheter via the right carotid artery [23,24]. Pacing was initiated above intrinsic heart rates using bipolar pacing electrodes in the right atrium, and was stepwise increased up to 600 bpm. The time constant for isovolumic relaxation, τ, was calculated as previously described [23] and left ventricular pressure tracings were fit to $P_t = P_o e^{-t/\tau}$, where P is pressure at time t (P_t) and at dP/dt_{min} (P_o).

2.7. In vivo echocardiography

2D guided M-mode echocardiography (9 MHz) and color-flow directed Doppler (5–7 MHz) were performed using an Interspec Apogee CX-200 ultrasonograph (Interspec-ATL, Ambler, PA) [24]. Mice were lightly anesthetized with 2.5% avertin (0.01 ml/g i.p.) and studies performed at baseline and after administration of isoproterenol (2.0 μg/g i.p.) [25].

2.8. Histopathologic and dot-blot analyses

Standard techniques were used for histological examination (Mason's trichrome sections) and dot-blot analysis of total RNA from left ventricles [18].

2.9. Materials

Type II collagenase (Worthington Biochemical). Antibodies were: PLB-monoclonal and calsequestrin-polyclonal (Affinity BioReagents); PS-16- and PT-17-polyclonal (PhosphoProtein Research); SERCA-polyclonal, which was generated in our laboratory.

2.10. Statistical analysis

Data are presented as mean±S.E.M. Statistical analysis was performed by Student's *t*-test for comparisons between two groups, and one-way or two-way ANOVA, followed by Student–Newman–Keuls' test, for multiple comparisons. $P<0.05$ was considered as statistically significant.

3. Results

3.1. Generation and identification of transgenic mice expressing mutant PLB/N27A in the phospholamban null background

Cardiac-specific expression of the PLB N27A mutant in the absence of endogenous wild-type PLB was achieved by mating transgenic mice overexpressing the mutant PLB/N27A with the PLB knockout mouse, previously generated in our laboratory. PCR analysis of tail genomic DNA was employed to identify the selected genotype (characterized by the presence of both the mutant PLB/N27A transgene and the neo gene, as well as the absence of endogenous PLB gene) using different sets of primers (Fig. 1). The presence of the mutant transgene was detected using a 5′-end α-MHCp-1 primer and a 3′-end PLB-RC primer corresponding to part of the transgenic construct to amplify an ~180 bp fragment. The presence of the neo gene, which was successfully used to replace part of the PLB gene in generating the PLB knockout mice in our laboratory, was identified using a 5′-end HLT7 primer corresponding to part of the PLB genomic sequence and a 3′-end neo 3 primer corresponding to part of the neo gene to amplify an ~550 bp fragment. Ablation of endogenous PLB was confirmed by absence of an ~650 bp PCR product using 5′-end HLT7 and 3′-end JS 940 primers corresponding to part of the PLB genomic sequence.

Quantitative immunoblotting of cardiac homogenates or SR-enriched membranes from mice expressing the mutant PLB/N27A in the PLB knockout background revealed no alterations in SERCA or calsequestrin protein levels in transgenic compared to wild-type hearts (Fig. 2A). The mutant PLB predominantly migrated as pentamers on SDS–PAGE, and dissociated to monomers upon boiling, similar to wild-type PLB. The levels of the mutant PLB were 1.11±0.11 in transgenic compared to wild-type

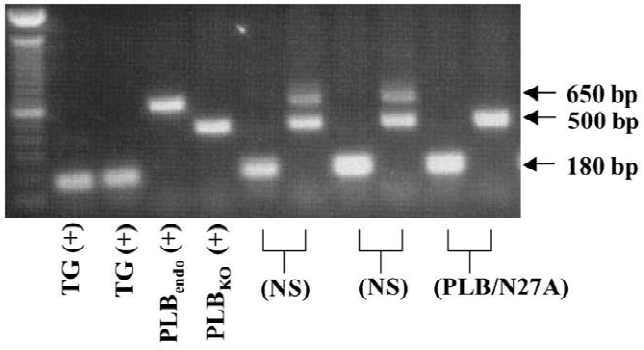

Fig. 1. Identification of transgenic mice expressing mutant PLB/N27A in the phospholamban null background. The presence of the transgene (TG) was identified by a 180-bp PCR product. The neo gene (PLB_{KO}) was recognized by a 500-bp PCR product. A 650-bp PCR product represents the endogenous PLB gene (PLB_{endo}). The selected genotype (PLB/N27A) is characterized by the presence of TG and PLB_{KO} genes, as well as the absence of PLB_{endo}. NS indicates the non-selected genotype.

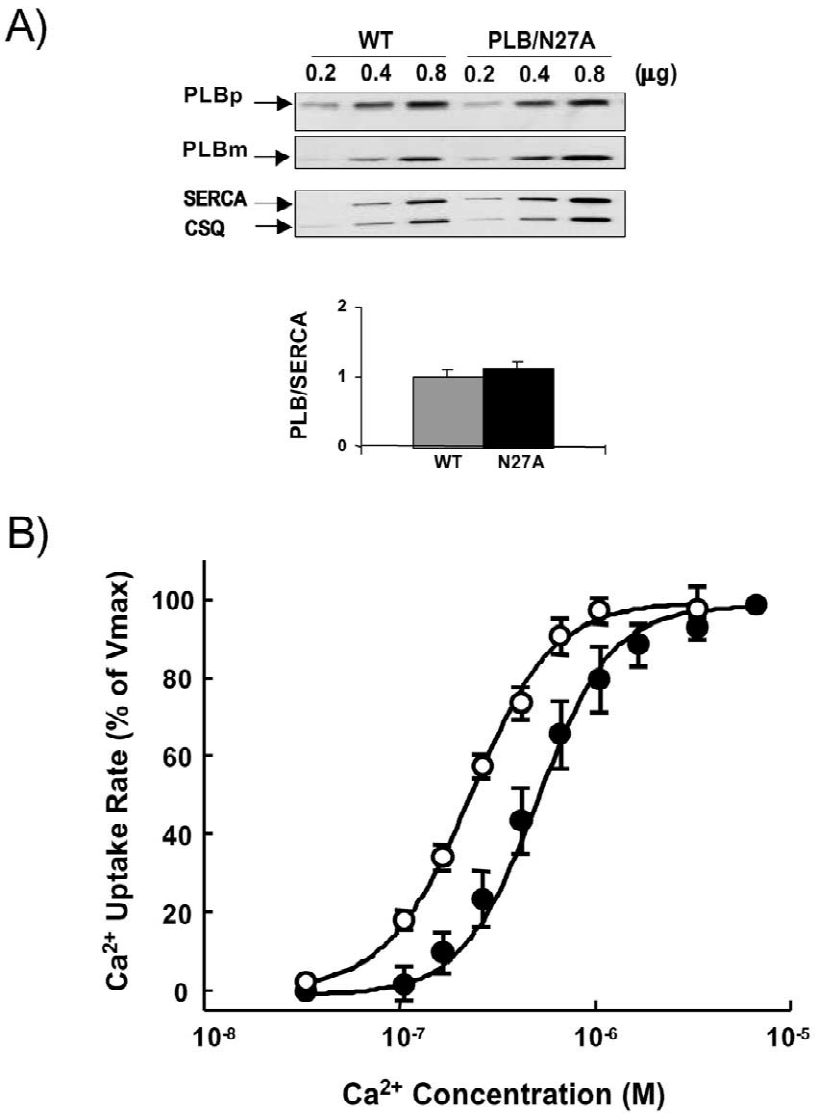

Fig. 2. Biochemical characterization of PLB/N27A hearts. (A) Representative quantitative immunoblots of cardiac SR enriched membranes probed with PLB, SR Ca^{2+}-ATPase (SERCA) or calsequestrin (CSQ) antibodies. 0.2, 0.4, and 0.8 μg protein were loaded to generate linear regression lines, and the slopes were used to compare the protein levels between wild type (WT; $n=5$) and PLB/N27A ($n=5$) hearts. PLBp and PLBm, pentameric and monomeric PLB. (B) The initial rates of oxalate-supported SR Ca^{2+} uptake in the PLB/N27A (●) and WT (○) hearts. Data are expressed as % of maximal uptake rates in each group. Values are mean±S.E.M. of five hearts, assayed in triplicate.

(1.00) hearts, resulting in a similar apparent PLB/SR Ca^{2+} ATPase ratio (1.08±0.16 in transgenic and 1.00 in wild-type). Furthermore, similar ratios of PLB/SR Ca^{2+} ATPase were observed in SR-enriched microsomal fractions from transgenic (0.84±0.13) and wild-type (1.00) hearts (Fig. 2A), indicating that the mutant PLB was incorporated into the SR membrane. ^{32}P-phosphorylation experiments by PKA catalytic subunit or Ca^{2+}/calmodulin-dependent protein kinase, revealed that the mutant PLB could be also phosphorylated to the same extent as wild-type PLB (data not shown).

To determine whether the mutant PLB could functionally interact with the SR Ca^{2+} ATPase, the initial rates of oxalate-facilitated SR Ca^{2+} uptake were assessed in cardiac homogenates (Fig. 2B). Expression of mutant PLB resulted in a rightward supershift of the EC_{50} of SR Ca^{2+} uptake (0.52±0.04 μM) compared to wild-types (0.21±0.01 μM). However, the maximal rates of Ca^{2+}-uptake in transgenic (49±7 nmol/mg/min) were not different from wild-type (48±3 nmol/mg/min) hearts.

3.2. Structural NMR analysis

The observed superinhibitory effects of PLB/N27A prompted us to examine its structure at the molecular level. Thus, wild-type and PLB/N27A peptides (AA 1–36) were synthesized, solubilized, and NMR spectra obtained. The N-terminal residues from V4 to I18 and the C-terminal residues from Q22 to F35 displayed an α-helical configuration (Fig. 3A). Analysis of the spectra of wild-type or

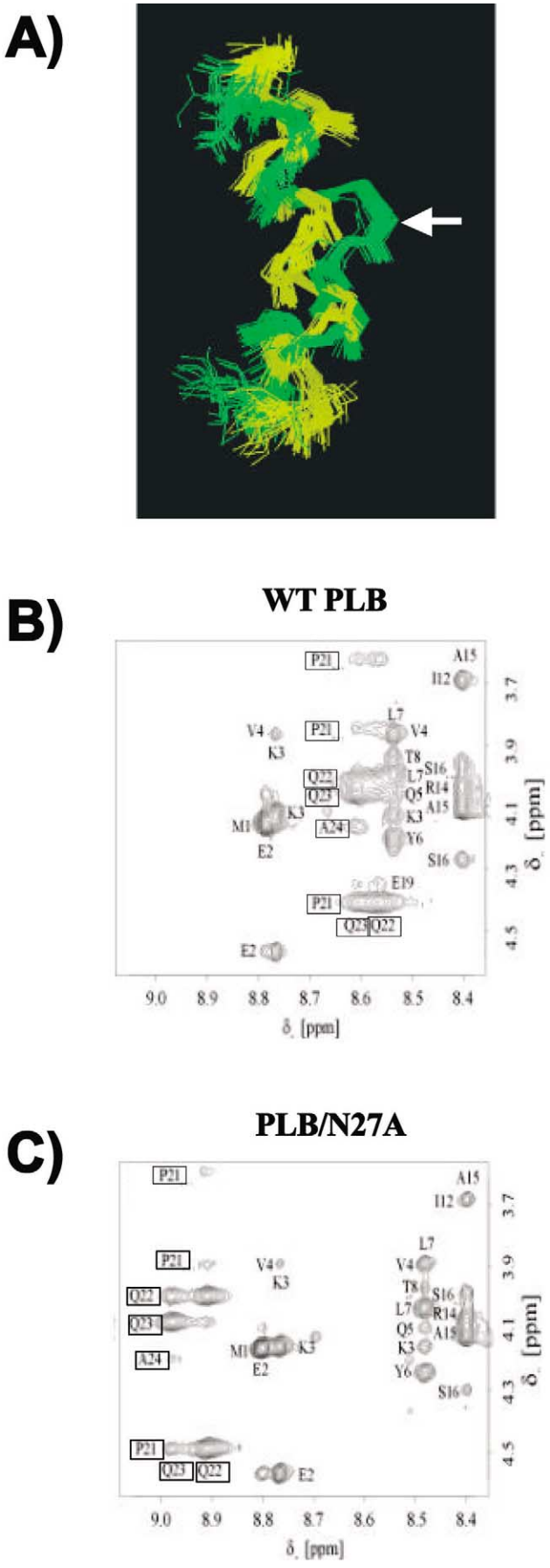

Table 1
Structural statistics

	WT	PLB/N27A
No. of structures[a]	40	40
RSMD		
M1–T17	1.15±0.62 Å	1.26±0.60 Å
M20–S36	1.09±0.38 Å	0.70±0.28 Å
Ramachandran (%)		
Favorable	59	73
Additional	32	23
Genereous	9	3
Disallowed	0	1
No. of restraints		
Total	899	922
Long	0	0
Medium	325	341
Short	349	357
Intra	225	224

[a] Forty structures were selected out of 200 computed on the basis of energy and restraints violations. RSMD, root square mean deviation calculated for the main chain heavy atoms; M1–T17, N-terminal helix of PLB 1–36; M20–S36, C-terminal helix of PLB 1–36; Ramachandran statistic, allowed region of the main chain torsion angles.

mutated peptide did not reveal the presence of multiple conformations in slow exchange. However, a clear difference was observed in the region adjacent to the mutation site, where the C-terminal helix of the mutant PLB/N27A adopted a different course compared to the wild-type (AA 20–36: Fig. 3A). This is of particular importance, since the mobility of this region has been suggested to play an important role in transmitting the effect of phosphorylation in domain Ia resulting in dissociation of the PLB/SERCA heterodimer. The structural statistics confirmed that the number of nOe cross peaks and the quality of the spectra were comparable for the two peptide families (Table 1). Fig. 3B and C display expansions of the NOESY spectra from wild-type and PLB/N27A peptides. Changes in the chemical shifts (P21–A24) were restricted to AA around the mutation, while the rest of the structure remained unaffected.

3.3. Functional measurements ex vivo

The decreased SERCA Ca^{2+}-affinity, observed at the subcellular level, was associated with functional alterations at the cellular level: rates of shortening and relengthening

Fig. 3. NMR studies. (A) Main chain atoms of the C-terminal helices from residues M20 to S36 are shown from families of 40 structures of mouse WT (green) and mutant PLB (yellow). (B and C) The figures are expansions of the proton nOe NMR spectra and represent only 2% of the whole spectral area. These expansions show the chemical shift changes of AA 21–24 in PLB/N27A (C) compared to WT PLB (B), from 1 mM samples dissolved in 30% TFE at pH 3.0. The low field ends of the spectra display correlations from the N-terminal residues of peptides and from the residues at the beginning of the C-terminal helix (Q22 to A24) adjacent to the loop region between the two helices, comprising residues from I18 to P21.

were significantly depressed to 67% and 54%, respectively, in PLB/N27A compared to wild-type (100%) myocytes. The Ca^{2+} transient kinetics also demonstrated a significant prolongation in the times for 50% (2.2-fold) and 80% (1.6-fold) decay of the Ca^{2+} signal in transgenic myocytes compared to wild-types (1.0-fold), reflecting impaired SR Ca^{2+} re-uptake. Since PLB has been shown to act as a key mediator of the cardiac response to β-agonists, myocytes were maximally stimulated with 300 nM isoproterenol. Interestingly, isoproterenol could not fully relieve the superinhibitory effects of PLB/N27A, and the maximally stimulated mechanical and Ca^{2+} kinetic parameters remained significantly depressed compared to wild-types (data not shown).

Similar to observations at the myocyte level, Langendorff perfusions indicated that the depressed contractile parameters in transgenic hearts under basal conditions (Fig. 4A and B), remained decreased under maximal β-agonist stimulation ($+dP/dt$ 52%; $-dP/dt$ 70%; time to half-relaxation, $RT_{1/2}$ 134%) compared to wild-types (100%). Phosphorylation of PLB, assessed by PLB phosphoserine or phosphothreonine site-specific antibodies, indicated that the phosphothreonine signal was significantly lower in transgenics, while the phosphoserine signal was similar to wild-types (Fig. 4C). These results suggested that the physiologically relevant site (Ser^{16}) for the isoproterenol stimulatory effects [19] was phosphorylated to the same extent in transgenic and wild-type hearts.

To examine the effects of mutant PLB-phosphorylation on SR function, ATP-dependent, oxalate-supported SR Ca^{2+} uptake was measured, using transgenic and wild-type hearts perfused in the absence or presence of isoproterenol (Fig. 4D). There were no significant differences in the maximal rates of Ca^{2+} uptake (V_{max}) among the four groups. Isoproterenol stimulation shifted the EC_{50} to the left of both wild-type and transgenic hearts, but the values

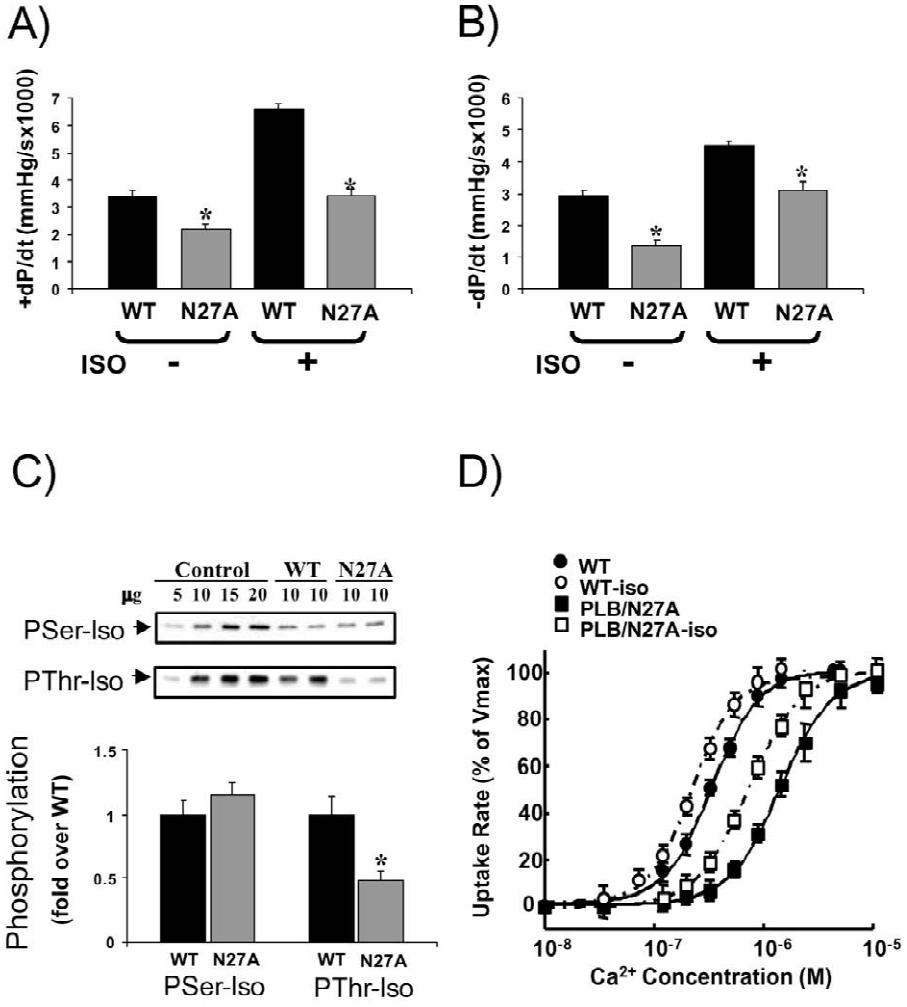

Fig. 4. Altered response to β-adrenergic stimulation. Langendorff-hearts were perfused in the presence of isoproterenol (1.0 μM) and frozen at the peak of the inotropic response. Basal (−) and isoproterenol-stimulated (+) values for (A) maximal rates of pressure development ($+dP/dt$) and (B) pressure decline ($-dP/dt$). (C) Phosphorylation of PLB, using PLB pSer and pThr site-specific antibodies. Quantification of pSer and pThr levels in PLB/N27A relative to WTs. (D) Isoproterenol (iso) effects on SR Ca^{2+} uptake in WT (EC_{50} 0.26±0.01 to 0.19±0.01 μM) and PLB/N27A (EC_{50} 1.00±0.10 to 0.52±0.01 μM) perfused hearts. Values are mean±S.E.M. ($n=5$). *$P<0.05$ vs. WT.

in transgenics remained higher, suggesting that phosphorylation of mutant PLB could not completely relieve its superinhibitory effects on the SR Ca^{2+} ATPase.

3.4. Invasive hemodynamics and contractile reserve in intact animals

To determine whether compensatory mechanisms may overcome the PLB inhibitory effects in vivo, hemodynamic parameters of mice were assessed using LV-catheterization (Fig. 5). At intrinsic heart rates (WT 402.4±11.0 vs. PLB/N27A 338.5±5.5; $P<0.05$), LV systolic pressure was preserved in PLB/N27A (Fig. 5A), but $+dP/dt$ was moderately decreased (Fig. 5B). Interestingly, diastolic parameters were significantly altered in the PLB/N27A hearts, as indicated by a doubling in LV end-diastolic pressure (Fig. 5C), and a significantly prolonged time constant for isovolumic left ventricular relaxation, τ (Fig. 5D). The response to β-adrenergic stimulation was also significantly attenuated (data not shown). To test whether PLB-superinhibition by PLB/N27A alters cardiac reserve, we examined the effect of heart rate on hemodynamic parameters. Incremental pacing resulted in a significant increase in the rate of contraction in hearts expressing wild-type PLB, but this frequency response was blunted in

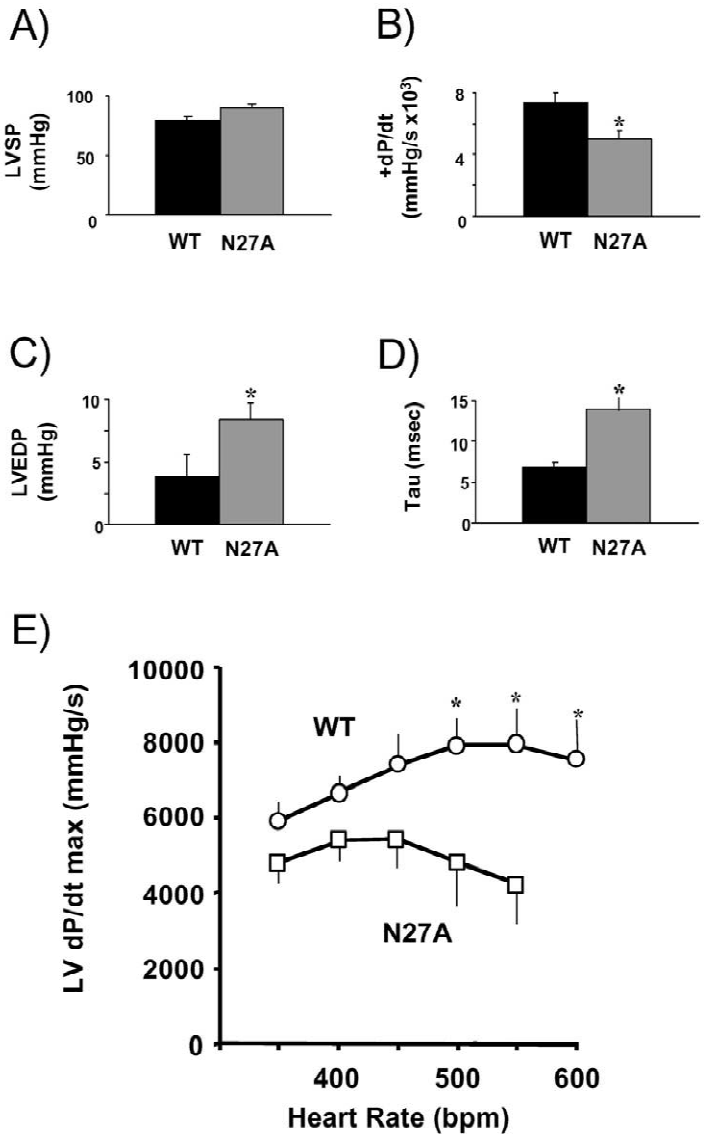

Fig. 5. Invasive hemodynamics in closed chest animals. Left ventricular indices are: (A) systolic pressure (LVSP), (B) rate of pressure development ($+dP/dt$), (C) left ventricular end diastolic pressure (LVEDP), and (D) time constant (τ) for relaxation. (E) Group data for force–frequency relationships from PLB/N27A and WT. For each group, data points denote maximal rates of contraction ($+dP/dt$ max) with increasing heart rates. Data are means±S.E.M. ($n=5$). bpm, beats per min. *$P<0.05$ versus WT.

Table 2
M-mode and Doppler echocardiographic measurements in PLB/N27A and wild-type mice

	WT		PLB/N27A	
	3 months	10 months	3 months	10 months
n	6	6	6	6
BW, g	31.6±1.2	37.5±2.3	35.5±2.0	34.9±3.1
EDD, mm	3.6±0.2	3.9±0.1	3.8±0.1	4.7±0.3*†
ESD, mm	2.2±0.1	2.4±0.10	2.4±0.2	3.4±0.2*†
PW Th, mm	0.7±0.1	0.7±0.04	0.8±0.05*	0.8±0.05
LVM_{cal}, mg	60.4±6.4	73.1±4.3	86.6±6.3*	129.8±18.4*†
LVM_{cal}/BW, mg/g	1.91±0.1	1.95±0.12	2.45±0.1*	3.71±0.5*†
h/r	0.37±0.01	0.35±0.03	0.42±0.02*	0.35±0.01†
FS, %	37.9±0.3	39.0±0.9	37.0±2.5	27.0±1.4*†
HR, bpm	363±32	450±9	232±20*	278.5±36*
Vcf_c, $circ^{-1}$	6.4±0.2	7.0±0.3	5.8±0.3	4.7±0.3*†
E/A	1.76±0.10	1.51±0.09	1.09±0.10*	1.97±0.43†
IVRT, ms	25.8±1.9	32.5±2.3	48.2±6.7*	54.5±5.3*

BW, body weight; EDD, end diastolic dimension; ESD, end systolic dimension; PW Th, posterior wall thickness; LVM_{cal}, calculated left ventricular mass; LVM/BW, calculated left ventricular mass/body weight; FS, fractional shortening; HR, heart rate; Vcf_c, velocity of circumferential shortening corrected for differences in heart rate; E/A, ratio of early to late diastolic transmitral velocity; IVRT, isovolumic relaxation time. Values are mean±S.E.M. of *n* animals. *$P<0.05$ vs. age-matched WT; †$P<0.05$ vs. 3-month PLB/N27A.

PLB/N27A hearts, as indicated by a leftward and downward shift of the force–frequency relation (Fig. 5E).

3.5. Effects of age

To assess the long-term effects of increased SERCA inhibition by PLB/N27A, non-invasive M-mode and Doppler echocardiography was employed (Table 2). In 3-month-old transgenic mice, heart rate was significantly lower, the ratio of early to late diastolic transmitral velocity was depressed, and the isovolumic relaxation time was significantly prolonged (187%), indicating the presence of impaired left ventricular relaxation. However, fractional shortening and velocity of circumferential fiber shortening, corrected for differences in heart rate, were not different in transgenic mice, suggesting that systolic function was compensated at a young age. Increases in end-diastolic posterior wall thickness to cavity ratio, and calculated LV/body mass indicated the presence of mild LV concentric hypertrophy in transgenic mice (Table 2). Cardiac hypertrophy (24%) was also confirmed by gravimetric analysis.

Despite this compensated LV dysfunction at 3 months of age, Kaplan–Meier analysis demonstrated that mutant mice died prematurely, between 10 and 15 months (Fig. 6A), reaching 50% of the cumulative survival rate at 13 months. Therefore, we examined transgenic animals at 10 months, the beginning of this period. There were further increases (90.3%) in calculated LV/body mass and LV geometry became eccentric by 10 months (Fig. 6B, Table 2). The increase in wall stress resulted in significant depression of systolic ejection phase indices (fractional shortening and velocity of circumferential fiber shortening), whereas there was no alteration in cardiac function of wild-type mice (Fig. 6C, Table 2). Besides deterioration of LV function in PLB mutants, a significant increase in lung/body weight ratios in PLB/N27A mice compared to wild-type was observed, indicative of lung congestion and decompensation of left heart failure (Fig. 6D). These structural and functional alterations were associated with reactivation of a fetal gene program, such as β-myosin heavy chain, skeletal α-actin, and ANF (Fig. 6E). Histopathological and gross examination revealed substantial interstitial fibrosis and hypertrophic myocytes in PLB/N27A hearts compared with no alterations in aging WT hearts (Fig. 7).

4. Discussion

To critically address the question of the role of PLB activity in the onset and progression of cardiomyopathy, the current study introduced a PLB mutant, which is a potent inhibitor of SERCA, in the null background. A single point-mutation of N27A in the hinge region of PLB caused a defined alteration in the 3-D structure of this regulatory protein, which was associated with increased inhibition of cytosolic Ca^{2+} sequestration by the SR Ca^{2+} ATPase. This translated into predominantly impaired relaxation in isolated myocytes, perfused hearts, and intact mice that eventually progressed to cardiac remodeling and congestive heart failure.

Since neither the native stoichiometry of PLB/SERCA nor the pentamer/monomer ratio was altered in this model, we hypothesized that a change in the structure of the mutant PLB/N27A might be the underlying mechanism of increased SERCA inhibition. Using NMR methodology, we demonstrated that mutant and wild-type PLB-peptides form N-terminal (V4 to I18) and C-terminal (Q22 to F35) α-helices connected by a turn, which is in agreement with

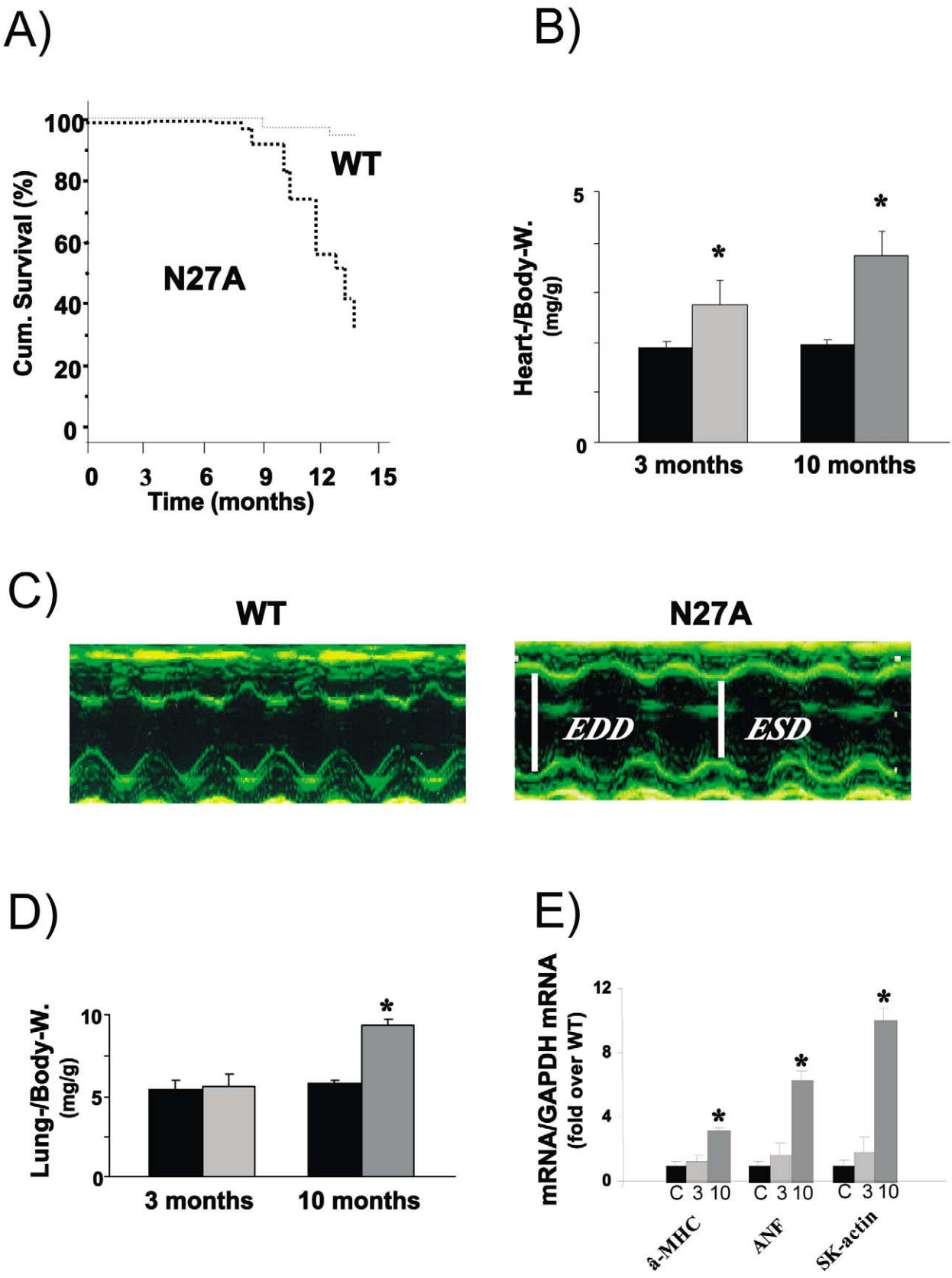

Fig. 6. Progressive remodeling and early mortality in aging N27A mice. (A) Kaplan–Meier survival curves comparing WT ($n=18$) and transgenic N27A ($n=13$) mice over a 14-month period. (B and D) Gravimetric analysis of biventricular and lung weights, respectively, of PLB/N27A (grey) and WT (black) mice. (C) Representative M-mode echocardiograms from 10-month-old WT and transgenic N27A hearts. (E) Quantitative grouped dot-blot analysis of ventricular RNA expression normalized to glyceraldehyde-3-phosphate dehydrogenase (GAPDH) in wild-type control (C) or 3-month (3) and 10-month (10) PLB/N27A hearts. Values are mean±S.E.M. ($n=6$). *$P<0.05$ versus WT.

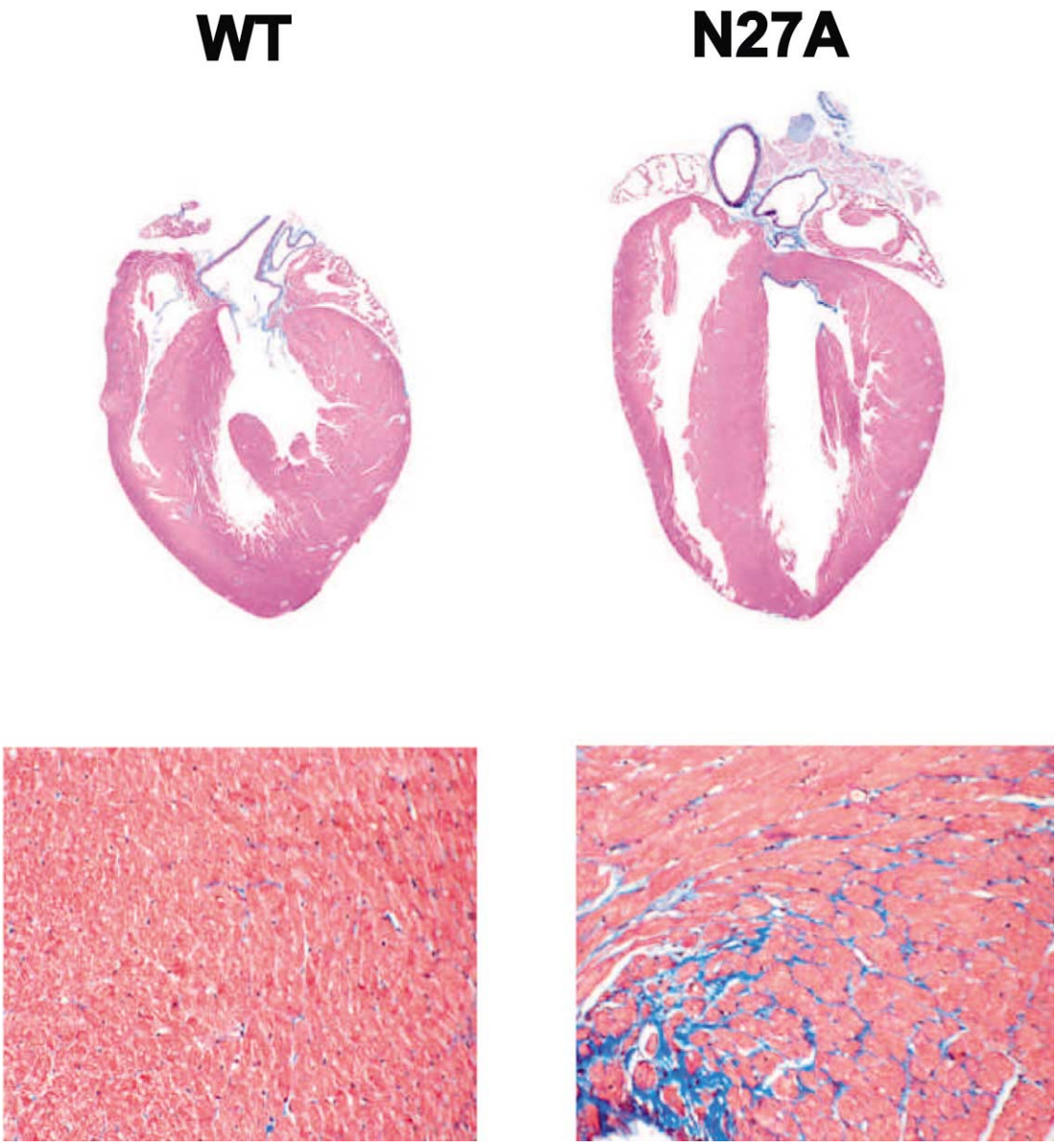

Fig. 7. Histopathology of WT and N27A hearts: representative Masson's trichrome staining for fibrosis (blue) in sectioned hearts from 10-month-old WT and mutant PLB/N27A mice (original magnification ×200). Upon aging, N27A hearts revealed interstitial fibrosis and myocyte hypertrophy.

previously published data by Pollesello et al. [20]. However, in the mutant peptide, the C-terminal helix adjacent to the site of the mutation was found to adopt a different course compared to wild-type. This structural alteration in PLB was likely associated with enhancement of its interaction with SERCA, possibly involving a long-range transmission among the PLB cytoplasmic and transmembrane domains [15]. Such enhanced association would be consistent with the increases (twofold) in the amount of SERCA co-immunoprecipitated with PLB/N27A [15] and the inability of phosphorylation, induced by β-agonists, to fully relieve the superinhibitory effects of PLB/N27A in vivo. Indeed, a change in mobility of the hinge domain has been proposed to be essential in transmitting the effects of phosphorylation in the cytoplasmic domain to the hydrophobic domain, resulting in dissociation of the PLB/SERCA heterodimer [20]. Furthermore, recent data suggest that a potential SERCA1-PLB interaction involves the cytoplasmic loop connecting M6 and M7 of SERCA1 (Asn810 to Asp813) and PLB domain IB (Asn27 and Asn30) [26]. Alternatively, pentameric PLB has also been proposed to form an ion pore in the SR membranes [27]. Nuclear magnetic resonance structure of PLB residues 1–36 revealed a clustering of glutamine and asparagine (Gln^{22}, Gln^{23}, Gln^{26} and Asn^{30}) lining the inner side of the cytoplasmic portion of pentameric PLB, and it was suggested that the polar residues in the cytoplasmic portion of PLB might modulate Ca^{2+} leakage from the SR thereby contributing to the inhibitory effect of PLB on SR Ca^{2+} sequestration [20]. It is therefore conceivable that pentameric PLB/N27A may exert some of its inhibitory effects by facilitating SR Ca^{2+} leakage. Interestingly, Asn27 in

PLB is the only amino acid, which is replaced by Lys in human (N27K), and this is associated with increased inhibitory function [15], suggesting that AA 27 in PLB may also account for functional differences among species.

In the current study, some of the effects of PLB/N27A expression on SR Ca^{2+} uptake and cardiac function in young adult mice qualitatively confirm results previously obtained in a mouse model overexpressing the mutant form in wild-type background [17]. However, the presence of endogenous PLB made it impossible to distinguish between the superinhibitory effect of the mutation and the impact of relative protein abundance. It was therefore mandatory to repeat those experiments in the knock-out background and in order to establish a causal relationship between the induction of a hinge region mutant, prolonged Ca^{2+} transients, contractile dysfunction and the initiation of progressive remodeling due to chronic SERCA inhibition. An interesting feature of the impaired SR Ca^{2+} sequestration in PLB/N27A hearts was a blunted force–frequency relation, observed in intact mice. Previous reports have indicated that the level of PLB and therefore, the magnitude of the SR Ca^{2+} loading is an important determinant of the force–frequency relation in intact mice [24,28]. Importantly, this impairment was found to precede LV dilation and heart failure in our model, consistent with clinical findings, where it appears to serve as an early marker for the transition from physiological to pathophysiological hypertrophy [29]. In this context it is noteworthy, that the phosphothreonine signal was significantly lower in PLB/N27A, while the phosphoserine signal was phosphorylated to the same extent in transgenic and wild-type hearts. Recent studies reported a decrease in Thr^{17} PLB phosphorylation in failing human myocardium [30]. Furthermore, frequency-dependent Thr^{17} PLB phosphorylation has been suggested to provide an intrinsic mechanism for cardiac myocytes to adapt to a sudden change in heart rate [31]. Thus, it could be hypothesized that a reduced ability of PLB/N27A to become phosphorylated at the $threonine^{17}$ site might contribute to the blunted frequency-dependent inotropic response in this model.

Several studies have proposed that impaired diastolic function may precede systolic dysfunction [2,32] and decreases in SERCA/PLB protein ratio or the degree of PLB phosphorylation are key characteristics in human and experimental heart failure [4,5,18]. Importantly, the current study documents that increased PLB inhibition of SERCA may be a critical early event for the initiation of compensated, predominantly LV diastolic dysfunction, which progresses to cardiac remodeling and congestive heart failure upon aging. It is thus reasonable to speculate, that if such a mutation were to occur in the human PLB gene, it would lead to a gain of PLB inhibitory function and cardiomyopathies, comparable to polymorphisms in structural or contractile proteins [9,33]. However, besides the diminished SR Ca^{2+} resequestration leading to inadequate filling of SR stores and Ca^{2+} available for subsequent contractions in PLB/N27A hearts, a number of secondary players may be activated and effect the transition from compensated to decompensated phase. One of these compensatory responses is the altered MHC-isoform expression, observed upon cardiac remodeling in the mutant hearts. Interestingly, cardiac overexpression of β-MHC induced neither hypertrophic remodeling nor heart failure in transgenic models [34], indicating that β-MHC alone is not a primary candidate for the PLB/N27A cardiac phenotype. Other secondary alterations may include depletion of energy-rich phosphates [2] and decreases in cyclic AMP levels [35]. The downstream molecular pathways that couple SR Ca defects to reprogramming of gene expression and initiation of the hypertrophic response in this and other models are currently unclear. Surprisingly, diastolic dysfunction preceded induction of fetal genes in PLB/N27A hearts, indicating that impaired SR Ca cycling may be a prime candidate for the activation of intrinsic hypertrophic signaling pathways, leading to cardiac remodeling. According to this view, improved SR Ca^{2+} sequestration by either downregulation [36], ablation of PLB [37] or overexpression of SERCA [38,39] was able to either prevent dilated cardiomyopathy [37] or reverse contractile dysfunction in myocytes from animal models or end-stage failing human hearts [36,38,39]. Longitudinal studies, employing gene expression profiling and proteomics in PLB/N27A hearts may delineate the cellular mechanisms involved in the transition from compensated diastolic dysfunction to combined diastolic and systolic heart failure.

In summary, the current study addresses the potential causative role of impaired SR Ca^{2+} cycling in diastolic dysfunction without major cardiac remodeling, and its progression to heart failure in vivo. The findings support the importance of the phospholamban/SERCA complex as a nodal point in the pathophysiology of dilated cardiomyopathy. Furthermore, it is conceivable that targeted disruption of the PLB hinge domain may be important in enhancing cardiac performance. Future studies on elucidating the precise mechanism of the hinge domain transmitting its regulatory effects on SERCA are warranted.

Acknowledgements

We are grateful to Ms. M. Nieman for excellent technical assistance, and Dr. P.R. Rosevear for critical discussions. This work was supported by NIH grants HL-26057, HL-64018, HL-52318, and P40RR12358 (E.G.K.), 5 T32 HL-07382 (A.C.), and HL-52318 (B.D.H).

References

[1] Morgan JP, Erny RE, Allen PD, Grossman W, Gwathmey JK. Abnormal intracellular calcium handling, a major cause of systolic and diastolic dysfunction in ventricular myocardium from patients with heart failure. Circulation 1990;81(2 Suppl):III21–32.

[2] Grossman W. Diastolic dysfunction in congestive heart failure. N Engl J Med 1991;325(22):1557–1564.
[3] Beuckelmann DJ, Nabauer M, Erdmann E. Intracellular calcium handling in isolated ventricular myocytes from patients with terminal heart failure. Circulation 1992;85(3):1046–1055.
[4] Hasenfuss G, Reinecke H, Studer R et al. Relation between myocardial function and expression of sarcoplasmic reticulum Ca(2+)-ATPase in failing and nonfailing human myocardium. Circ Res 1994;75(3):434–442.
[5] Schwinger RH, Munch G, Bolck B, Karczewski P, Krause EG, Erdmann E. Reduced Ca(2+)-sensitivity of SERCA 2a in failing human myocardium due to reduced serin-16 phospholamban phosphorylation. J Mol Cell Cardiol 1999;31(3):479–491.
[6] Perez NG, Hashimoto K, McCune S, Altschuld RA, Marban E. Origin of contractile dysfunction in heart failure: calcium cycling versus myofilaments. Circulation 1999;99(8):1077–1083.
[7] Gomez AM, Valdivia HH, Cheng H et al. Defective excitation–contraction coupling in experimental cardiac hypertrophy and heart failure. Science 1997;276(5313):800–806.
[8] Marx SO, Reiken S, Hisamatsu Y et al. PKA phosphorylation dissociates FKBP12.6 from the calcium release channel (ryanodine receptor): defective regulation in failing hearts. Cell 2000;101(4):365–376.
[9] Li D, Tapscoft T, Gonzalez O et al. Desmin mutation responsible for idiopathic dilated cardiomyopathy. Circulation 1999;100(5):461–464.
[10] Luo W, Grupp IL, Harrer J et al. Targeted ablation of the phospholamban gene is associated with markedly enhanced myocardial contractility and loss of beta-agonist stimulation. Circ Res 1994;75(3):401–409.
[11] Kadambi VJ, Ponniah S, Harrer JM et al. Cardiac-specific overexpression of phospholamban alters calcium kinetics and resultant cardiomyocyte mechanics in transgenic mice. J Clin Invest 1996;97(2):533–539.
[12] Wegener AD, Simmerman HK, Lindemann JP, Jones LR. Phospholamban phosphorylation in intact ventricles. Phosphorylation of serine 16 and threonine 17 in response to beta-adrenergic stimulation. J Biol Chem 1989;264(19):11468–11474.
[13] Cornea RL, Autry JM, Chen Z, Jones LR. Re-examination of the role of the leucine/isoleucine zipper residues of phospholamban in inhibition of the Ca^{2+}-pump of cardiac sarcoplasmic reticulum. J Biol Chem 2000;275(52):41487–41494.
[14] Toyofuku T, Kurzydlowski K, Tada M, MacLennan DH. Amino acids Glu2 to Ile18 in the cytoplasmic domain of phospholamban are essential for functional association with the Ca(2+)-ATPase of sarcoplasmic reticulum. J Biol Chem 1994;269(4):3088–3094.
[15] Kimura Y, Asahi M, Kurzydlowski K, Tada M, MacLennan DH. Phospholamban domain Ib mutations influence functional interactions with the Ca2+-ATPase isoform of cardiac sarcoplasmic reticulum. J Biol Chem 1998;273(23):14238–14241.
[16] Zvaritch E, Backx PH, Jirik F et al. The transgenic expression of highly inhibitory monomeric forms of phospholamban in mouse heart impairs cardiac contractility. J Biol Chem 2000;275(20):14985–14991.
[17] Zhai J, Schmidt AG, Hoit BD et al. Cardiac-specific overexpression of a superinhibitory pentameric phospholamban mutant enhances inhibition of cardiac function in vivo. J Biol Chem 2000;275(14):10538–10544.
[18] Dash R, Kadambi VJ, Schmidt AG et al. Interactions between phospholamban and beta-adrenergic drive may lead to cardiomyopathy and early mortality. Circulation 2001;103(6):889–896.
[19] Luo W, Chu G, Sato Y et al. Transgenic approaches to define the functional role of dual site phospholamban phosphorylation. J Biol Chem 1998;273(8):4734–4739.
[20] Pollesello P, Annila A, Ovaska M. Structure of the 1–36 amino-terminal fragment of human phospholamban by nuclear magnetic resonance and modeling of the phospholamban pentamer. Biophys J 1999;76(4):1784–1795.
[21] Wüthrich K. NMR of proteins and nucleic acids. New York: John Wiley, 1986.
[22] Guntert P, Mumenthaler C, Wuthrich K. Torsion angle dynamics for NMR structure calculation with the new program DYANA. J Mol Biol 1997;273(1):283–298.
[23] Lorenz JN, Kranias EG. Regulatory effects of phospholamban on cardiac function in intact mice. Am J Physiol 1997;273(6 Pt 2):H2826–2831.
[24] Kadambi VJ, Ball N, Kranias EG, Walsh RA, Hoit BD. Modulation of force–frequency relation by phospholamban in genetically engineered mice. Am J Physiol 1999;276(6 Pt 2):H2245–2250.
[25] Hoit BD, Khoury SF, Kranias EG, Ball N, Walsh RA. In vivo echocardiographic detection of enhanced left ventricular function in gene-targeted mice with phospholamban deficiency. Circ Res 1995;77(3):632–637.
[26] Asahi M, Green M, Kurzydlowski K, Tada M, MacLennan DH. Phospholamban domain IB forms an interaction site with the loop between transmembrane helices M6 and M7 of sarco(endo)plasmic reticulum Ca2+ ATPase. Circulation 2001;104(17 Suppl):240, Abstract.
[27] Simmerman HK, Kobayashi YM, Autry JM, Jones LR. A leucine zipper stabilizes the pentameric membrane domain of phospholamban and forms a coiled-coil pore structure. J Biol Chem 1996;271:5941–5946.
[28] Pieske B, Maier LS, Bers DM, Hasenfuss G. Ca^{2+} handling and sarcoplasmic reticulum Ca^{2+} content in isolated failing and nonfailing human myocardium. Circ Res 1999;85(1):38–46.
[29] Inagaki M, Yokota M, Izawa H et al. Impaired force–frequency relations in patients with hypertensive left ventricular hypertrophy. A possible physiological marker of the transition from physiological to pathological hypertrophy. Circulation 1999;99(14):1822–1830.
[30] Munch G, Bolck B, Karczewski P, Schwinger RH. Evidence of calcineurin-mediated regulation of SERCA 2a activity in human myocardium. J Mol Cell Cardiol 2002;34(3):321–334.
[31] Hagemann D, Kuschel M, Kuramochi T et al. J Biol Chem 2000;275(29):22532–22536.
[32] Brutsaert DL, Sys SU. Relaxation and diastole of the heart. Physiol Rev 1989;69(4):1228–1315.
[33] Seidman CE, Seidman JG. Molecular genetic studies of familial hypertrophic cardiomyopathy. Basic Res Cardiol 1998;93(Suppl 3):13–16.
[34] Tardiff JC, Hewett TE, Factor SM et al. Expression of the beta (slow)-isoform of MHC in the adult mouse heart causes dominant-negative functional effects. Am J Physiol Heart Circ Physiol 2000;278(2):H412–419.
[35] Feldman MD, Copelas L, Gwathmey JK et al. Deficient production of cyclic AMP: pharmacologic evidence of an important cause of contractile dysfunction in patients with end-stage heart failure. Circulation 1987;75(2):331–339.
[36] del Monte F, Harding SE, William Dec G, Gwathmey JK, Hajjar R. Targeting phospholamban by gene transfer in human heart failure. Circulation 2002;105:904–907.
[37] Minamisawa S, Hoshijima M, Chu G et al. Chronic phospholamban-sarcoplasmic reticulum calcium ATPase interaction is the critical calcium cycling defect in dilated cardiomyopathy. Cell 1999;99(3):313–322.
[38] del Monte F, Harding SE, Schmidt U et al. Restoration of contractile function in isolated cardiomyocytes from failing human hearts by gene transfer of SERCA2a. Circulation 1999;100(23):2308–2311.
[39] Schmidt U, del Monte F, Miyamoto MI et al. Restoration of diastolic function in senescent rat hearts through adenoviral gene transfer of sarcoplasmic reticulum Ca(2+)-ATPase oxalate-supported Ca^{2+} uptake in SR. Circulation 2000;101(7):790–796.